surrounding liquid instead of accelerating molecular diffusion may result in arising segregated structures in the system [24,28,35]. This is probably the main reason why decreasing viscosity of the base solution elevates the final selectivity in the semi-batch reactor. In the case of no flow instabilities in the system one would rather expect an opposite effect.

### 7.3. Modelling of Micromixing in the Semi-Batch Reactor.

The model of concentration moments proposed in chapter 5.1 was applied to interpret the experimental results and determine energetic efficiency of mixing in the semi-batch reactor. According to this model, the selectivity of competitive-parallel reactions:

$$A + B \overset{k_1}{\rightarrow} P \qquad \text{with} \quad k_1 \rightarrow \infty \,, \tag{5.34a}$$

$$A + C \overset{k_2}{\rightarrow} Q \qquad \text{and} \quad R_i = -k_2 \cdot c_A \cdot c_C \tag{5.34b}$$

depends on five dimensionless parameters:

- volume ratio $a = V_{(B,C)0} / V_{A0}$ , (5.42b)

- stoichiometric ratios $F_B = N_{B0} / N_{A0}$ , $F_C = N_{C0} / N_{A0}$ , (5.42c)

- characteristic times ratio $\theta = t_D / t_F$ , (5.42d)

- Damköhler number $\overline{Da} = k_2 \cdot \overline{c_{A0}} \cdot t_D = k_2 \cdot \dfrac{c_{A0}}{a+1} \cdot t_D$ . (5.49)

For the case of the test reactions (6.1), symbols **A**, **B** and **C** represent NaOH, HCl and $CH_2ClCOOC_2H_5$, respectively. Values of **a**, $\mathbf{F_i}$ and $\overline{\mathbf{c}}_{\mathbf{A0}}$ depend on volumes of mixed solutions and initial concentrations of the reactants in these solutions. The rate constant of alkaline hydrolysis was taken as for water solution at 25°C ($k_2$=33.2 $dm^3/(mol \cdot s)$ [77]) - see results presented in chapter 6.4.

The characteristic diffusion time, appearing in expressions (5.42d) and (5.49) is given by

$$t_D = \delta_0^2 / D_A \,. \tag{5.43}$$

The diffusivity coefficient of sodium hydroxide can be calculated from empirical correlation (6.14); for the solutions used in the experiments one receives $D_A = 6.28 \cdot 10^{-10}$ $m^2/s$.

The visual observations of the feeding stream coloured with phenolphthalein showed that for

$\mathbf{n} \geq 50$ rev/min and $\mathbf{Q_f} \leq 2$ cm$^3$/min the feeding stream had a shape of a thin ribbon, swept from the tip of the dosing pipe, carried downward to the turbine along a spiral trajectory and thrown away by the turbine in the radial direction. In this case, using a continuity relation one can assume that the initial size of the feeding stream is related to the feeding rate, $\mathbf{Q_f}$, and the velocity of a liquid in the close surrounding of the outlet, **v**, in the following way:

$$s_0 = \sqrt{12} \cdot \delta_0 \sim Q_f / \mathrm{v} \ . \tag{7.3}$$

The characteristic fluid mechanical time, appearing in expression (5.42d), is related to the average deformation rate $\overline{\alpha}$ of the liquid elements in the reaction zone:

$$t_F = 1/\overline{\alpha} \ . \tag{7.4}$$

The deformation rate at any material point $\vec{\mathbf{X}}$ in the system depends on the rate of energy dissipation per unit volume and energetic efficiency of mixing - see chapter 2.4:

$$\alpha(\vec{X},t) = eff(\vec{X},t) \cdot \sqrt{\frac{\epsilon}{2 \cdot \mu}} \ . \tag{7.5}$$

Averaging $\alpha$ over lifetime of the limiting reactant **A** in the system yields:

$$\overline{\alpha} = \frac{1}{t_f} \cdot \int_0^{t_f} eff(\vec{X},t) \cdot \sqrt{\frac{\epsilon}{2 \cdot \mu}} \, dt = \overline{eff(t_f) \cdot \sqrt{\phi}} \cdot \sqrt{\frac{\langle \epsilon \rangle_V}{2 \cdot \mu}} \ , \tag{7.6}$$

where factor $\phi$ relates the local value of $\epsilon$ to the mean power input per unit volume in the mixer:

$$\epsilon = \phi \cdot \langle \epsilon \rangle_V \ . \tag{7.7}$$

The mean rate of energy dissipation per unit volume

$$\langle \epsilon \rangle_V = \frac{4 \cdot P}{\pi \cdot D^2 \cdot H} = \frac{4 \cdot P}{27 \cdot \pi \cdot d^3} \tag{7.8}$$

can be determined from the experimental correlation between the power number

$$Po = \frac{P}{d^5 \cdot n^3 \cdot \rho} \tag{7.9}$$

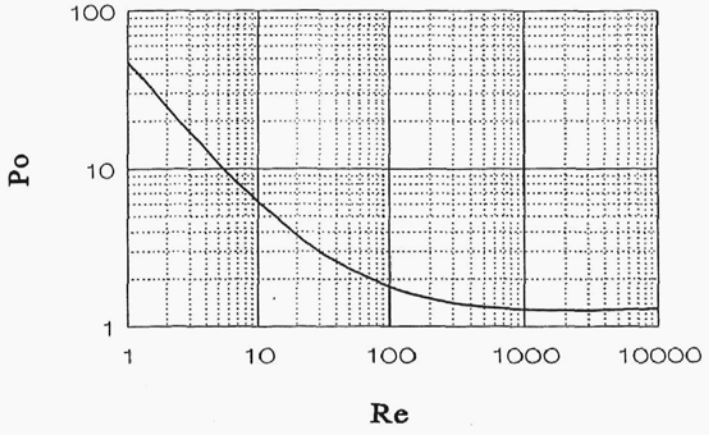


**Figure 7.6. Power curve for the semi-batch reactor.**

and the stirrer Reynolds number plotted in figure 7.6 [83]. This relationship was obtained for the geometrical configuration of the mixer used in the experiments. For **Re** ranging from 1 to 740 one can use the approximate expression:

$$\log_{10} Po = 1.687 - 1.080 \cdot \log_{10} Re + 0.185 \cdot (\log_{10} Re)^2 \ . \qquad \textbf{(7.10)}$$

Eventually, knowing $\langle \epsilon \rangle_V$ one can relate the average efficiency of mixing $\overline{\mathrm{eff}(t_f) \cdot \sqrt{\phi}}$ in the reaction zone to the model parameter $\bar{\alpha}$ using equation (7.6). It should be pointed out, however, that efficiency $\overline{\mathrm{eff}(t_f) \cdot \sqrt{\phi}}$ refers to the average power input per unit volume. Only when $\phi$ is known can one relate $\bar{\alpha}$ to $\overline{\mathrm{eff}(t_f)}$.

Efficiency of mixing $\overline{\mathrm{eff}(t_f) \cdot \sqrt{\phi}}$ and the ratio $s_0/Q_f$ were determined by fitting computed selectivities to the experimental points shown in figure 7.2 (n=100 rev/min, a=19). The aim of this procedure was to minimize the expression:

$$\sigma_6 = \sqrt{\frac{1}{6} \cdot \sum_{i=1}^{i=6} \left[ \frac{X_{model}(Q_{fi}) - X(Q_{fi})}{X(Q_{fi})} \right]^2} \ , \qquad \textbf{(7.11)}$$

where $\mathbf{X_{model}(Q_{fi})}$ and $\mathbf{X(Q_{fi})}$ are the selectivities computed and measured for six feeding rates $Q_{fi}[cm^3/min]=\{0.18,0.25,0.385,0.5,1.0,2.0\}$. As the result, the best matching was obtained for:

$$\overline{eff(t_f) \cdot \phi^{0.5}} = 0.05 \qquad \textbf{(7.12a)} \qquad \text{and} \qquad [s_0/Q_f]_{n=1.67\,rev/s} = 2760 \ s/m^2 \ . \qquad \textbf{(7.12b)}$$

Comparison of the theoretical curve with the experimental points is shown in figure 7.7. The agreement is very good ($\sigma_6$=3.93%) except one point obtained for the shortest feeding time. The initial values of the slab thickness calculated from equation (7.12b) were ranging from 0.008 to 0.092 mm. These results prove that the feeding stream was subjected to rapid deformation just behind the outlet of the dosing pipe.

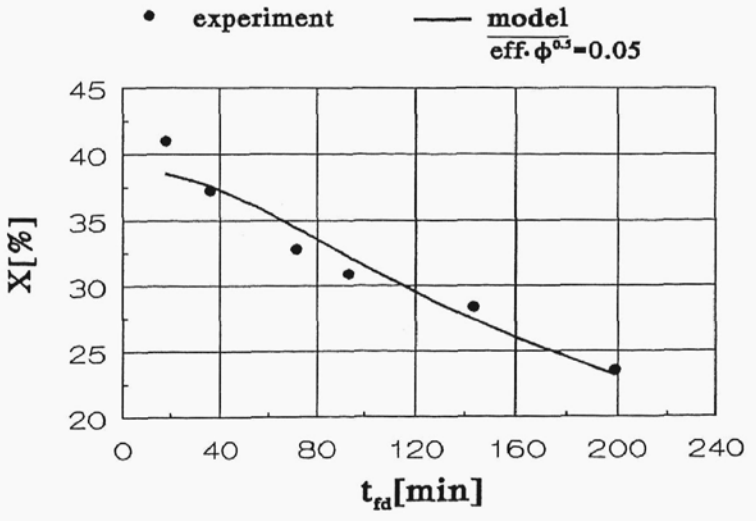


**Figure 7.7. Effect of the feeding time on the final selectivity for the semi-batch reactor; n=100 rev/min, a=19.**

The high value of efficiency determined in the computations shows that the reaction zone

must have been localized near the agitator. In this area, local rates of energy dissipation per unit volume considerably exceed the average value of power input per unit volume in the whole reactor ($\phi$>1).

According to expression (7.3) the value of ratio $\mathbf{Q_f/s_0}$ should be proportional to the liquid velocity close to the feeding point. This velocity should in turn depend on the revolution speed of the pitched-blade turbine. Taking it into account, the relation between the ratio $\mathbf{Q_f/s_0}$ and the revolution speed, **n**, was expressed as follows:

$$\frac{[s_0/Q_f]_{n=n_2}}{[s_0/Q_f]_{n=n_1}} = \left(\frac{n_1}{n_2}\right)^{\gamma} . \qquad (7.13)$$

Finally, making use of relation (7.12b) determined for **n**=100 rev/min one receives:

$$\frac{s_0}{Q_f} = 2760 \cdot \left(\frac{1.67}{n}\right)^{\gamma} \quad [s/m^2] . \qquad (7.14)$$

Fitting of the model parameters to experimental results for **n**=400 rev/min, **a**=19 and $\mathbf{Q_f}$=1 cm$^3$/min, gives $\gamma$=1.5. Figure 7.8 shows that for the revolution speeds other than 100 and 400 rev/min the agreement between the experimental points and the model predictions is also satisfactory when $\gamma$ equal to 1.5 is used in equation (7.4).

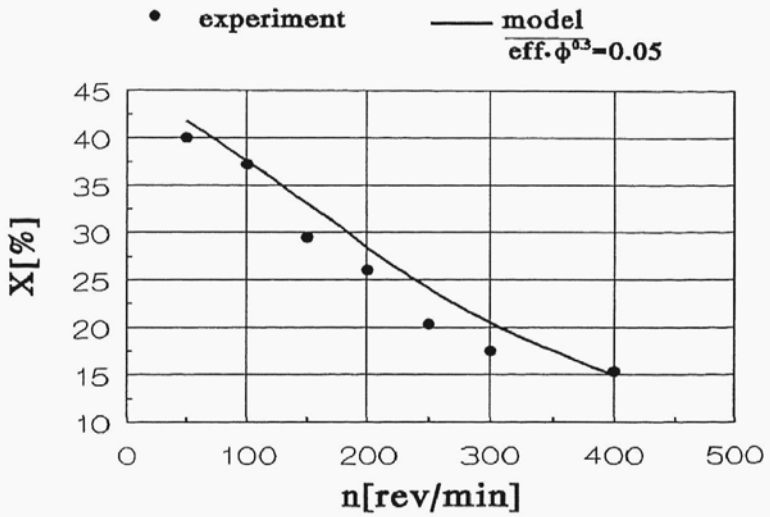


**Figure 7.8. Effect of the revolution speed on the final selectivity for the semi-batch reactor; a=19, $\mathbf{Q_f}$=1 cm$^3$/min.**

The $\gamma$ value is higher than one; this indicates that for the investigated range of the revolution speeds of the pitched-blade turbine (**3<Re<24**) the dimensionless liquid velocity, $\mathbf{v/(\pi \cdot n \cdot d)}$, in the region close to the feeding point depends on Reynolds number. Only in the creeping flow regime and for well developed turbulent flow should one expect $\mathbf{v/(\pi \cdot n \cdot d)} \neq f(Re)$.

The experiments revealed that decreasing the volume ratio **a**, improves mixing in the semi-batch reactor. Figures 7.9ab show that the model correctly predicts this effect. Similarly as in the experiments, the influence of **a** on the product distribution was found stronger for higher agitation speed.

Slightly worse agreement was found between the experimental points obtained for different feeding rates and the model predictions in the case when **n**=400 rev/min and **a=19** - see figure 7.10. Summarizing, one can see that the model of concentration moments allows to determine efficiency of mixing, which characterizes both the mixer and the method of feeding; the values of efficiency obtained by fitting the model constants to experimental data refer only to that region of the mixer where mixing proceeds by chemical reaction. It should also be noted that the model correctly predicts the effect of the agitation speed, the feeding time and the volume ratio on the product distribution.

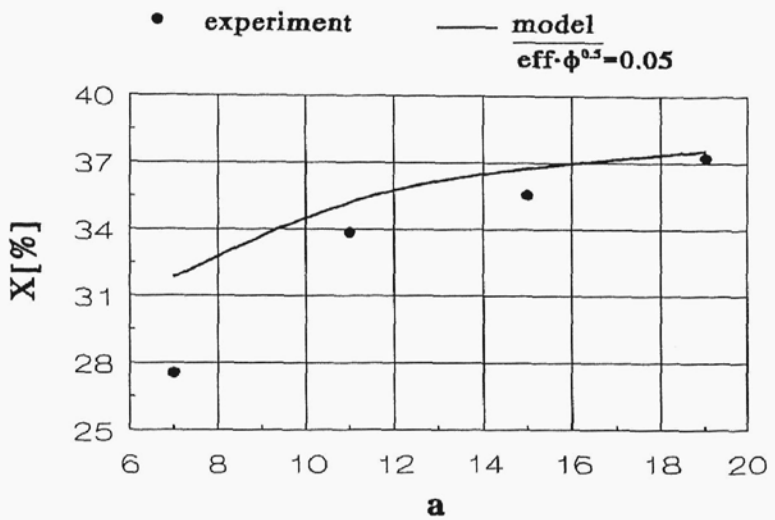


**Figure 7.9a. Effect of the volume ratio on the selectivity for the semi-batch reactor; n=100 rev/min, $Q_f$=1 cm$^3$/min.**

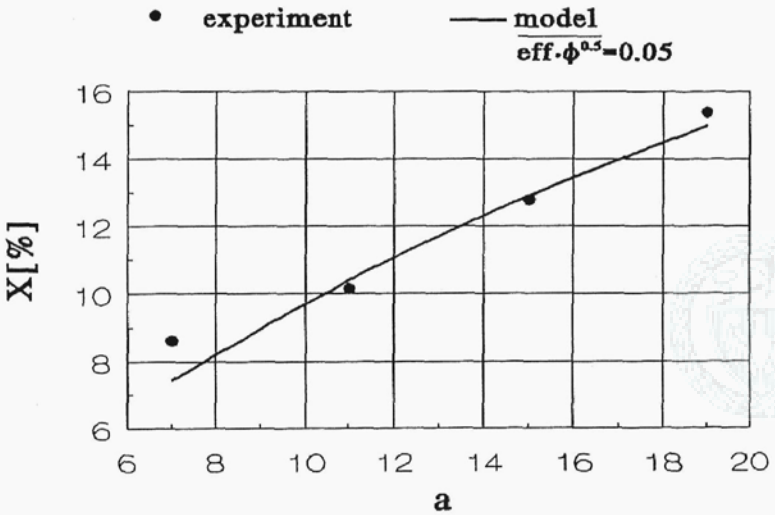


**Figure 7.9b. Effect of the volume ratio on the selectivity for the semi-batch reactor; n=400 rev/min, $Q_f$=1 cm$^3$/min.**

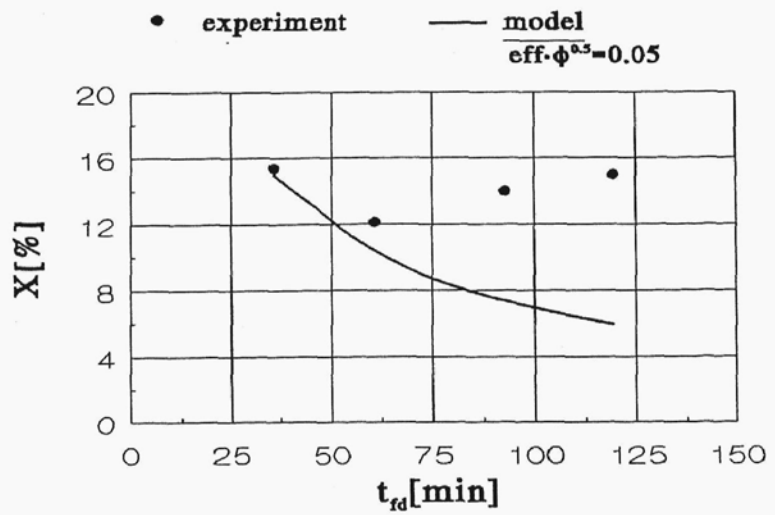


**Figure 7.10. Effect of the feeding time on the selectivity for the semi-batch reactor; n=400 rev/min, a=19.**